Titration of Tertiapin-Q Inhibition of ROMK1 Channels by Extracellular Protons†

Yajamana Ramu, Angela M. Klem, and Zhe Lu*

Department of Physiology, University of Pennsylvania, 3700 Hamilton Walk, Philadelphia, Pennsylvania 19104

Received November 8, 2000; Revised Manuscript Received January 12, 2001

ABSTRACT: Tertiapin-Q (TPN_Q), a honey bee toxin derivative, inhibits inward-rectifier K^+ channels by binding to their external vestibule. In the present study we found that TPN_Q inhibition of the channels is profoundly affected by extracellular pH. This pH dependence mainly reflects titration of histidine residue 12 in TPN_Q by extracellular protons, since it largely vanishes when the histidine residue is replaced with alanine. Not surprisingly, this alanine derivative of TPN_Q binds to the channel with much lower affinity. Quantitative thermodynamic cycle analysis shows that deprotonation of the histidine residue reduces the TPN_Q−ROMK1 binding energy by 1.6 kcal/mol. To eliminate pH sensitivity but retain high affinity, we derivatized TPN_Q by replacing histidine 12 with lysine. This derivative—denoted tertiapin-KQ (TPN_{KQ})—not only is practically insensitive to extracellular pH but also binds to the channel with even higher affinity than TPN_Q at extracellular pH 7.6.

Tertiapin (TPN), a 21 residue protein originally isolated from honey bee venom, inhibits the cardiac GIRK1/4 and the renal ROMK1 inward-rectifier K^+ channels with nanomolar affinity (*1*). However, in cardiac myocytes TPN inhibition of the muscarinic receptor-controlled GIRK1/4 channels appears to be specific (*2*; for GIRK1/4 channels see refs *3* and *4*). TPN interacts with the inward-rectifier K^+ channels with one to one stoichiometry and inhibits the channel by binding to its external vestibule (*5*).

The C-terminal portion (histidine 12 to glycine 19) of TPN adopts an α-helical structure, whereas its N-terminal half acquires extended conformations (*6*). TPN binds to the channel primarily through its α-helix (*5*). Methionine residue 13, located at the N-terminal end of the α-helix, readily undergoes oxidation under ambient conditions, and the oxidation significantly hinders the binding of TPN (*7*). This technical inconvenience of TPN can be circumvented by replacing methionine 13 with glutamine to yield a TPN derivative called tertiapin-Q or TPN_Q (*7*). TPN_Q though nonoxidizable under ambient conditions binds to the channels with TPN-like affinity and selectivity.

In the present study we found that the binding of TPN_Q to the channel is dramatically affected by extracellular pH and, therefore, investigated how extracellular protons affect TPN_Q binding. We have also produced a TPN_Q derivative that not only is practically extracellular pH-insensitive but also binds to the channel with even higher affinity at extracellular pH 7.6.

MATERIALS AND METHODS

Synthesis of ROMK1 cRNA and Its Expression in Xenopus Oocytes. The ROMK1 cDNA was cloned into a pSPORT plasmid (Gibco-BRL) (*8*). The cRNA was synthesized using T7 polymerase (Promega) from the cDNA linearized with *Not*I.

Oocytes harvested from *Xenopus laevis* frogs were digested with collagenase (2 mg/mL) in a solution containing NaCl, 82.5 mM, KCl, 2.5 mM, $MgCl_2$, 1 mM, and HEPES, 5 mM (pH 7.6) and agitated on a platform shaker at 80 rpm for 90 min. The oocytes were then rinsed thoroughly with and stored in a solution containing: gentamicin, 50 μg/mL, NaCl, 96 mM, KCl, 2 mM, $CaCl_2$, 1.8 mM, $MgCl_2$, 1 mM, and HEPES, 5 mM (pH 7.6). Defolliculated oocytes were selected at least 2 h after the collagenase digestion. To express the ROMK1 channels, the coding RNA was injected into oocytes. All injections were carried out at least 16 h after the collagenase treatment. The injected oocytes were stored at 18 °C.

Channel Recording. The ROMK1 channels were studied using a two-electrode voltage clamp amplifier (Oocyte Clamp OC-725C, Warner Instruments Corp.). The resistance of electrodes filled with 3 M KCl was 0.2−0.4 MΩ. To elicit current through the channels, the oocyte membrane potential was stepped to −80 mV and then to +80 mV from a holding potential of 0 mV. Background leak currents were obtained by exposing oocytes to solutions containing >1 μM TPN_Q. The background current insensitive to TPN_Q, whose amplitude is comparable to that in oocytes uninjected with cRNA, does not inwardly rectify. The bath solution contained K^+ ($Cl^- + OH^-$), 100 mM, $CaCl_2$, 0.3 mM, $MgCl_2$, 1 mM, and HEPES, 10 mM (at specified pH adjusted with KOH). The concentrations of all TPN derivatives were calculated by converting the absorbance of the solution at 280 nm using the extinction coefficient 6.1 mM^{-1} cm^{-1} (*1*). All TPN derivatives used in the experiments were synthetic (see below).

Synthesis, Mass Determination, and Purification of Tertiapin Derivatives. TPN derivatives were synthesized using a Rainin/Protein Technologies Symphony multipeptide syn-

† This study was supported by NSF Grant IBN-97-27436. Z.L. was a recipient of an NIH Independent Scientist Award (HL03814).

* To whom correspondence should be addressed. E-mail: zhelu@mail.med.upenn.edu.

10.1021/bi002584n CCC: $20.00
Published on Web 03/03/2001

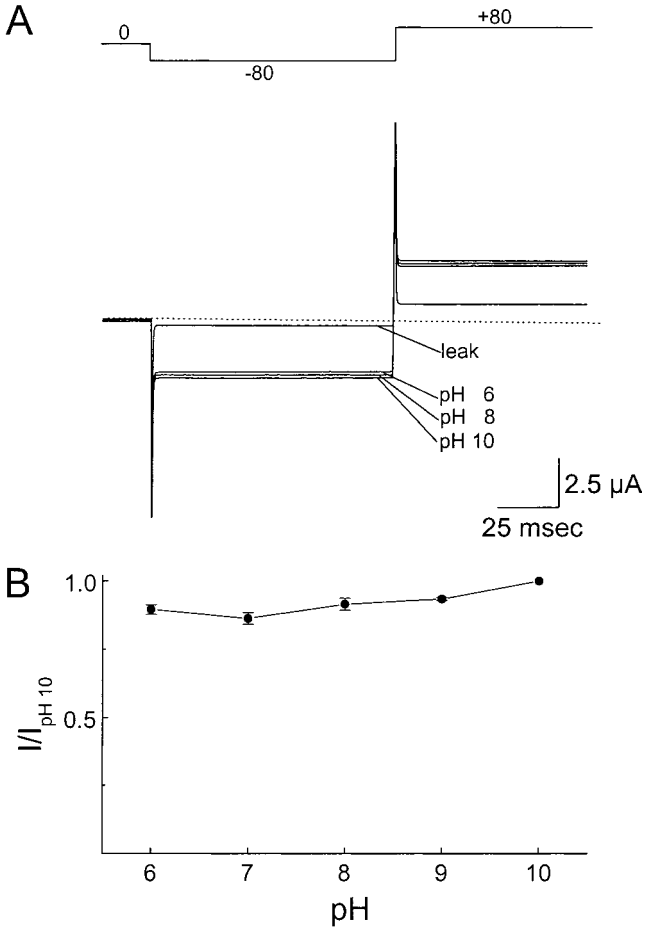

FIGURE 1: ROMK1 currents at various extracellular pH values. (A) ROMK1 current traces at three values of extracellular pH, elicited by the voltage protocol shown. The leak current trace was obtained in the presence of >1 μM TPN_Q. The dotted lines identify the zero current level. (B) Currents normalized to that at pH 10 (mean ± SEM, $n = 5$) are plotted against the corresponding extracellular pH.

thesizer, and their mass was confirmed on a VG analytical MALDI-TOF spectrometer (Keck Biopolymer Facility, Yale University). All synthetic TPN derivatives have a C-terminal amide group. Each synthetic peptide was dissolved in a solution containing 1 mM DTT and 10 mM Tris (pH 8.0). After DTT became oxidized, the peptide spontaneously adopted the active conformation and was purified on a reverse-phase HPLC column (C18) using a linear methanol gradient (1% per minute) (*1*).

RESULTS

Effect of Extracellular pH on the ROMK1 Current. Figure 1A shows macroscopic current traces of the ROMK1 channels at three representative extracellular pH values, elicited by the voltage protocol shown. The mean channel currents are plotted against pH in Figure 1B; all current values are normalized to that for pH 10. The channel current increased only slightly with increasing pH, consistent with a previous observation in a related channel, IRK1 (*9*).

Titration of TPN_Q Binding to ROMK1 Channels by Extracellular Protons. Figure 2A−C shows current traces of the ROMK1 channels without and with TPN_Q at three extracellular pH values. The concentration of TPN_Q needed to reduce the current by half increased significantly with

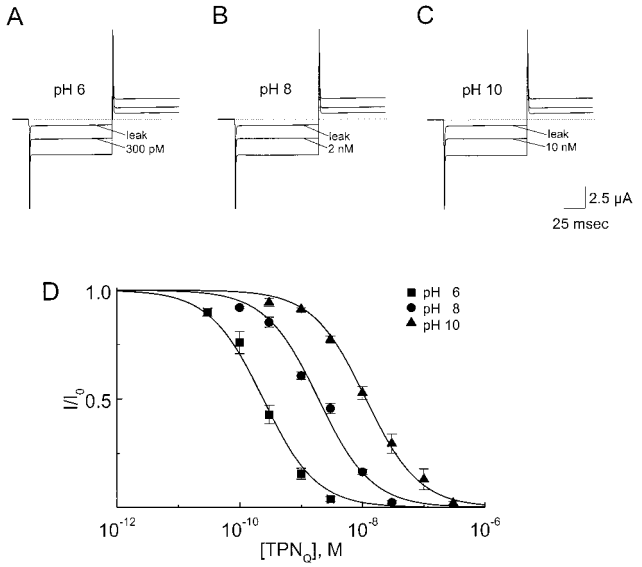

FIGURE 2: Inhibition of ROMK1 channels by TPN_Q at various extracellular pH values. (A−C) Current traces of ROMK1 channels at extracellular pH 6, 8, or 10 in the absence and presence of TPN_Q at the concentrations indicated. Voltage protocol was as in Figure 1. (D) The fraction of unblocked currents (mean ± SEM, $n = 5$) at each pH is plotted as a function of TPN_Q concentration. The curves superimposed on the data points are fits of the equation $I/I_0 = K_d/(K_d + [TPN_Q])$. The K_d values determined from the fits are summarized in Figure 6A.

increasing pH. The fraction of unblocked current as a function of TPN_Q concentration at the three pH values is shown in Figure 2D. The fitted curves, which assume that one TPN_Q molecule inhibits one channel, yield equilibrium dissociation constants (K_d) for the TPN_Q−ROMK1 complex at the three pH values tested. Raising the pH from 6 to 10 increased the K_d value by about 40-fold. (For a plot of K_d versus pH see Figure 6A.)

Effects of Mutations in TPN_Q on the Titration of the TPN_Q−ROMK1 Interaction by Extracellular Protons. We wondered whether the effect of extracellular pH on TPN_Q binding reflects proton titration of the histidine (residue 12) in TPN_Q, whose unperturbed pK_a value should be near neutral pH. Alanine substitution for histidine 12 causes the largest reduction in binding energy of the TPN_Q−ROMK1 complex among all substitutions for non-cysteine residues (*5*; see Figure 6B for TPN structure model). To test our idea, we examined how replacing histidine with nontitratable alanine affects the proton titration of TPN_Q binding. Figure 3A−C shows ROMK1 current traces at three values of extracellular pH, in the absence or presence of a TPN_Q with an alanine mutation at residue 12—denoted tertiapin-AQ (TPN_{AQ}). At pH 6 and 8, 30 nM TPN_{AQ} inhibited about half of the ROMK1 current, while a slightly higher concentration (100 nM) was required at pH 10. Figure 3D plots the fraction of unblocked current at each of the three pH values as a function of TPN_{AQ} concentration. The curves superimposed on the data are fits of an equation which assumes that one TPN_{AQ} molecule inhibits one channel. The K_d of TPN_{AQ} is practically the same for pH 6 and 8 and is only about 3-fold higher even at pH 10. These findings support the idea that the extracelluar pH titration of TPN_Q binding is largely due to a titration of histidine 12 in TPN_Q.

Our finding implies that the positive charge in the side chain of residue 12 is critical for high-affinity binding of

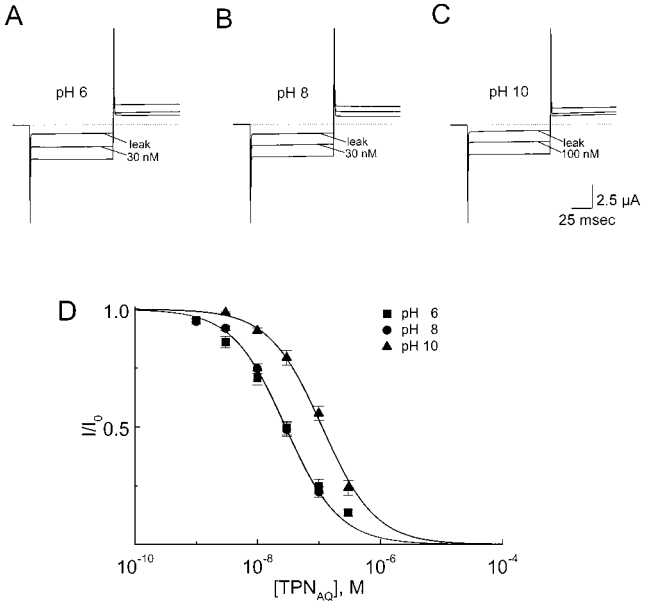

FIGURE 3: Inhibition of ROMK1 channels by TPN_{AQ} at various extracellular pH values. (A−C) ROMK1 current traces at extracellular pH 6, 8, or 10 in the absence and presence of TPN_{AQ} at the concentrations indicated. (D) The fraction of unblocked currents (mean ± SEM, $n = 5$) at each pH is plotted as a function of TPN_{AQ} concentration. The curves superimposed on the data points are fits of the equation $I/I_0 = K_d/(K_d + [TPN_{AQ}])$. The K_d values determined from the fits are summarized in Figure 6A.

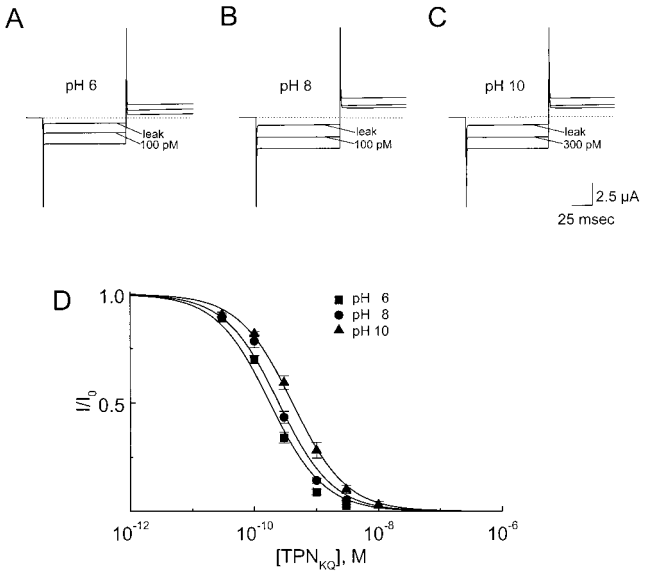

FIGURE 4: Inhibition of ROMK1 channels by TPN_{KQ} at various extracellular pH values. (A−C) ROMK1 current traces at extracellular pH 6, 8, or 10 in the absence and presence of TPN_{KQ} at the concentrations indicated. (D) The fraction of unblocked currents (mean ± SEM, $n = 5$) at each pH is plotted as a function of TPN_{KQ} concentration. The curves superimposed on the data points are fits of the equation $I/I_0 = K_d/(K_d + [TPN_{KQ}])$. The K_d values determined from the fits are summarized in Figure 6A.

TPN_Q to ROMK1. To test this, we replaced the histidine residue with another basic residue, lysine, which has a much higher pK_a. Figure 4A−C shows ROMK1 current traces in the absence and presence of TPN_Q with a lysine mutation at residue 12—denoted tertiapin-KQ (TPN_{KQ}). At pH 6 and 8, as little as 100 pM TPN_{KQ} inhibits about half of the current, and a 3-fold higher concentration (300 pM) was required at pH 10, as was the case for TPN_{AQ}. In Figure 4D the fraction

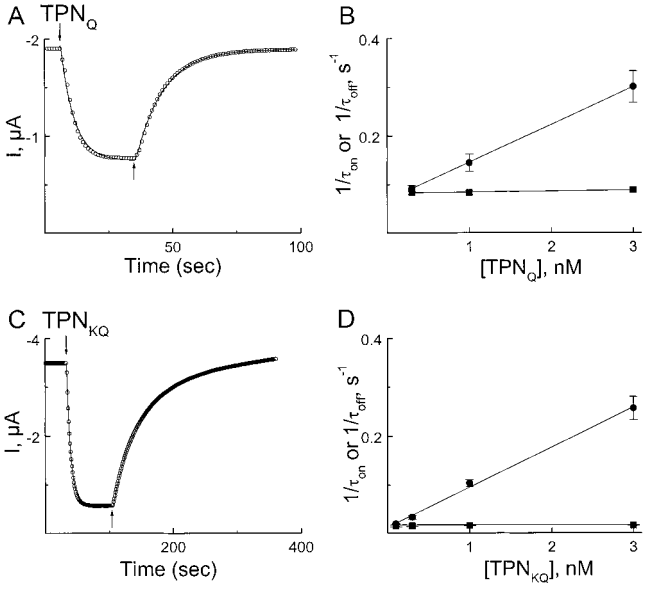

FIGURE 5: Kinetics of ROMK1 channel inhibition by TPN_Q and TPN_{KQ}. (A, C) Time courses of current changes upon washing in and washing out 1 nM TPN_Q and TPN_{KQ}, respectively. The starting time of washing in and washing out is indicated by a down arrow and an up arrow, respectively. The smooth curves superimposed on the data points are single-exponential fits. (B, D) The reciprocals of time constants (mean ± SEM, $n = 5$) for washing in ($1/\tau_{on}$, closed circles) as well as washing out ($1/\tau_{off}$, closed squares) are plotted as a function of TPN_Q and TPN_{KQ} concentration, respectively. The lines superimposed on the data are fits of the equations $1/\tau_{on} = k_{on}[TPN_Q] + k_{off}$ and $1/\tau_{off} = k_{off}$. The fits yield that $k_{on} = 7.74\ (\pm 0.52) \times 10^7\ M^{-1}\ s^{-1}$ [mean (±SEM), $n = 5$] and $k_{off} = 8.31\ (\pm 0.15) \times 10^{-2}\ s^{-1}$ for TPN_Q and that $k_{on} = 8.19\ (\pm 0.30) \times 10^7\ M^{-1}\ s^{-1}$ and $k_{off} = 1.35\ (\pm 0.48) \times 10^{-2}\ s^{-1}$ for TPN_{KQ}.

of unblocked current at each pH is plotted against the concentration of TPN_{KQ}. The curves are fits of an equation which assumes that one TPN_{KQ} molecule inhibits one channel. Like that of TPN_{AQ}, the K_d of TPN_{KQ} is practically the same at pH 6 and 8 and is only about 3-fold larger even at pH 10, although its K_d value is about 300-fold lower than that of TPN_{AQ}.

Effect of Lysine Mutation at Residue 12 on the Kinetics of the TPN_Q−ROMK1 Interaction. Figure 5A shows the time course of current inhibition upon addition, and then removal, of 1 nM TPN_Q at pH 7.6 (at which most of the previous toxin studies were performed). The smooth curves superimposed on the data points are single-exponential fits. The reciprocals of time constants for washing in and washing out of TPN_Q ($1/\tau_{in}$ and $1/\tau_{out}$), determined as shown in Figure 5A, are plotted in Figure 5B against TPN_Q concentration. The value of $1/\tau_{in}$ depends linearly on the concentration of TPN_Q whereas $1/\tau_{out}$ is concentration independent, as expected for a one to one binding stoichiometry between TPN_Q and ROMK1. From the slope of the plot of $1/\tau_{in}$ versus TPN_Q concentration and $1/\tau_{out}$, we determined the rate constants of TPN_Q binding and unbinding (k_{on} and k_{off}) as $7.74 \times 10^7\ M^{-1}\ s^{-1}$ and $8.31 \times 10^{-2}\ s^{-1}$, respectively.

For comparison, we also examined the kinetics of channel inhibition by TPN_{KQ}. Figure 5C shows the time course of current inhibition upon addition, and then removal, of 1 nM TPN_{KQ}. The smooth curves superimposed on the data points are single-exponential fits. The values of $1/\tau_{in}$ and $1/\tau_{out}$, determined from the fits as shown in Figure 5C, are plotted in Figure 5D against the concentration of TPN_{KQ}. Like those

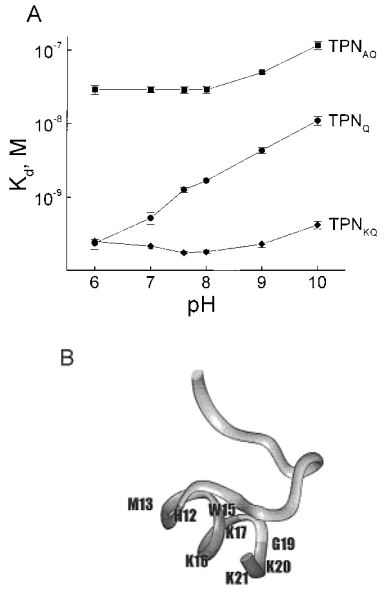

FIGURE 6: (A) Equilibrium dissociation constants of TPN derivatives at various extracellular pHs. The K_d values (mean ± SEM; $n = 5$) of TPN_Q (closed circles), TPN_{AQ} (closed squares), and TPN_{KQ} (closed diamonds), determined as shown in Figures 2−4, are plotted against extracellular pH. (B) Ribbon representation of the NMR structure model of TPN (*6*), where the positions of the eight C-terminal non-cysteine residues are indicated.

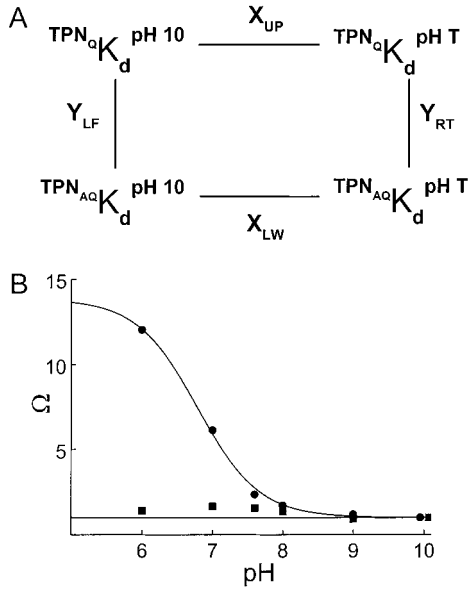

FIGURE 7: Thermodynamic cycle analysis of energetic coupling between histidine 12 in TPN_Q and extracellular protons. (A) Thermodynamic cycle. K_ds at the four corners of the thermodynamic cycle box are those of TPN_Q at pH 10 (upper left), TPN_Q at test pH T (upper right), TPN_{AQ} at pH 10 (lower left), and TPN_{AQ} at test pH T (lower right), where pH 10 is the reference for other pHs. X_{UP} and X_{LW} are the ratios of the horizontally adjacent K_d values, while Y_{LF} and Y_{RT} are the ratios of the vertically adjacent K_d values. The ratio of X_{UP}/X_{LW} (or Y_{LF}/Y_{RT}) is defined as Ω. (B) Closed circles represent Ω values for TPN_Q versus TPN_{AQ} at various extracellular pHs, whereas closed squares are those for TPN_{KQ} versus TPN_{AQ}. The curve superimposed on the closed circles is a fit of the equation $\Omega = (\Omega_{max} - \Omega_{min})/(1 + 10^{pH-pK_a}) + \Omega_{min}$, where Ω_{min} is one which is identified by the horizontal line. The fit yields $pK_a = 6.8$ and $\Omega_{max} = 13.8$. Since for both of the cases the Ω value is unity at pH 10, for clarity the two symbols were separated horizontally.

of TPN_Q, the value of $1/\tau_{in}$ of TPN_{KQ} varies linearly with the concentration of TPN_{KQ} while that of $1/\tau_{out}$ is concentration independent. The determined values of k_{on} and k_{off} for TPN_{KQ} are 8.19×10^7 M^{-1} s^{-1} and 1.35×10^{-2} s^{-1}, respectively. Thus, the increased affinity of TPN_Q for ROMK1 due to the lysine mutation results almost entirely from a decrease in the dissociation rate of the complex.

DISCUSSION

Tertiapin-Q inhibits ROMK1 by binding to the channel's external vestibule. The affinity of TPN_Q for ROMK1 is significantly reduced at high extracellular pH. This extracellular proton titration of the TPN_Q−ROMK1 interaction is mainly mediated by histidine 12 in TPN_Q, since the observed extracellular pH dependence is largely eliminated when histidine is replaced by a non-pH-titratable residue.

As shown in Figure 6A, the K_d of TPN_Q increases (>40-fold) from 0.25 nM at pH 6 to 11 nM at pH 10. By comparison, the K_d values of the mutants TPN_{AQ} and TPN_{KQ} (which differ by over 100-fold) vary only 3-fold in the same pH range. The observed effect of extracellular pH on TPN_Q binding must therefore result mainly from a titration of histidine 12 in TPN_Q and also, to a much lesser extent, from the titration of additional sites (channel or toxin) between pH 8 and 10. It should be noted that the ROMK1 channel itself is somewhat sensitive to extracellular protons, as shown by the small current enhancement as the pH is raised from 8 to 10 (Figure 1). Therefore, the small rise in the K_d of TPN_Q and its derivatives, observed in that extracellular pH range, may reflect titration of (a) site(s) in the channel itself.

To remove this small background pH dependence of the TPN_Q−ROMK1 interaction and isolate the energetic component solely related to the titration of the histidine residue from our analysis of the behavior of the histidine residue proper, we used thermodynamic cycle analysis (*10*−*12*). Since the two interacting elements of interest are histidine 12 in TPN_Q and extracellular protons, the two variables of the thermodynamic cycle are (1) the nature of residue 12 (e.g., histidine versus alanine) and (2) extracellular pH. Therefore, the dissociation constants (K_d) at the four corners of the thermodynamic cycle box (Figure 7A) are those of TPN_Q at pH 10 (upper left), TPN_Q at test pH T (upper right), TPN_{AQ} at pH 10 (lower left), and TPN_{AQ} at test pH T (lower right), where pH 10 is the reference pH. X_{UP} and X_{LW} are the ratios of the (upper and lower) horizontally adjacent K_d values, while Y_{LF} and Y_{RT} are the ratios of the (left and right) vertically adjacent K_d values. The ratio X_{UP}/X_{LW} (or ratio Y_{LF}/Y_{RT}) is defined as Ω (*10*). The natural logarithm of Ω represents the difference in protonation-related free energy change (in RT units) between the TPN_Q−ROMK1 complex with histidine and the TPN_Q−ROMK1 complex with alanine at position 12. Since alanine substitution eliminates the protonation site (shaving, as it were, the imidazole ring off the histidine side chain), the variation in the value of Ω reflects only the extent of protonation of the histidine side chain, despite the fact that the alanine mutation affects the TPN_Q−ROMK1 interaction also by other mechanisms unrelated to the protonation, as discussed below.

In Figure 7B, Ω values (closed circles), which were computed using the mean K_d values shown in Figure 6A, are plotted against the corresponding values of extracellular pH. The value of Ω increased by 12-fold when pH was

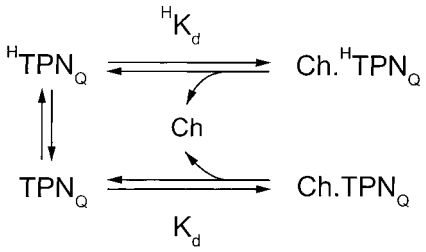

FIGURE 8: Minimal model for how protonation of histidine 12 affects TPN_Q binding to the channel. In the model, TPN_Q may exist in one of two states, $^HTPN_Q$ or TPN_Q, depending on whether histidine 12 is protonated. $^HTPN_Q$ and TPN_Q bind to the channel (Ch) with equilibrium dissociation constants ^HK_d and K_d, respectively.

lowered from 10 to 6. A fit of the data with an equation described in Figure 7B yields a pK_a for the titrated group of 6.8—well within the range expected for the pK_a of an unperturbed histidine side chain. The maximal Ω value estimated from the fit is 13.8. Thus, protonation of histidine 12 increases the binding energy by 1.6 kcal/mol. As a control we tested TPN_{KQ}, in place of TPN_Q, against TPN_{AQ}. Since an alanine residue is nontitratable and a lysine residue (pK_a ≈ 11) remains largely protonated between pH 6 and 10, the Ω value of TPN_{KQ} against TPN_{AQ} is expected to be near unity throughout the entire pH range (*10*). This is indeed what we observe (Figure 7B, square symbols).

The scheme in Figure 8 represents a minimal model for how protonation affects TPN_Q binding to the channel. In the model, TPN_Q may exist in one of two states, $^HTPN_Q$ or TPN_Q, depending on whether histidine 12 (pK_a = 6.8) is protonated. The binding of $^HTPN_Q$ or TPN_Q to the channel (Ch) is characterized by the equilibrium dissociation constants ^HK_d and K_d. According to the scheme, the observed equilibrium dissociation constant of TPN_Q at a given pH (K_{d-obs}) is given by

$$K_{d-obs} = \frac{1}{\frac{\theta}{^HK_d} + \frac{1-\theta}{K_d}} \quad (1)$$

where

$$\theta = \frac{1}{1 + 10^{pH-pK_a}} \quad (2)$$

which argues that the K_{d-obs} for TPN_Q would indeed vary sigmoidally with pH were it not for the additional background pH effect.

Since the pK_a of histidine 12 is 6.8, the residue should be largely protonated at pH 6 and practically fully deprotonated at pH 10. At low pH, the K_d value for TPN_{KQ} is very similar to that for TPN_Q, which suggests that TPN_{KQ} energetically resembles protonated TPN_Q (Figure 6A). Certainly, TPN_{KQ} has some experimentally beneficial features: (1) its binding to the channel is practically insensitive to extracellular pH, and (2) its affinity for the channel is even higher at the commonly used pH 7.6 (0.18 versus 1.26 nM), which is almost entirely due to a slower off-rate. On the other hand, TPN_{AQ} is quite different from deprotonated TPN_Q, since the K_d value for TPN_Q is still 10-fold smaller than that for TPN_{AQ} even at pH 10 where histidine 12 should practically be fully deprotonated. Therefore, although the positive charge in the side chain of the histidine residue is critical for the high-affinity binding of TPN_Q to the channel, other properties of the side chain also influence the TPN_Q—ROMK1 interaction. This phenomenon is not surprising since the toxin histidine residue appears to interact intimately with the channel (*5*).

ACKNOWLEDGMENT

We thank K. Ho and S. Hebert for the ROMK1 cDNA clone and P. De Weer for critical review of the manuscript.

REFERENCES

1. Jin, W., and Lu, Z. (1998) *Biochemistry 37*, 13291−13299.
2. Kitamura, H., Yokoyama, M., Akita, H., Matsushita, K., Kurachi, and Yamada, M. (2000) *J. Pharmacol. Exp. Ther. 293*, 196−205.
3. Kubo, Y., Reuveny, E., Slesinger, P. A., Jan, Y. N., and Jan, L. Y. (1993) *Nature 364*, 802−806.
4. Krapivinsky, G., Gordon, E. A., Wickman, K., Velimirovic, B., Krapivinsky, L., and Clapham, D. E. (1995) *Nature 374*, 135−141.
5. Jin, W., Klem, A. M., Lewis, J. H., and Lu, Z. (1999) *Biochemistry 38*, 14294−14301.
6. Xu, X., and Nelson, J. W. (1993) *Proteins: Struct., Funct., Genet. 17*, 124−137.
7. Jin, W., and Lu, Z. (1999) *Biochemistry 38*, 14286−14293.
8. Ho, K., Nichols, C. G., Lederer, W. J., Lytton, J., Vassilev, P. M., Kanazirska, M. V., and Hebert, S. C. (1993) *Nature 362*, 31−38.
9. Yang, J., Yu, M., Jan, Y. N., and Jan, L. Y. (1997) *Proc. Natl. Acad. Sci. U.S.A. 94*, 1568−1572.
10. Hidalgo, P., and MacKinnon, R. (1995) *Science 268*, 307−310.
11. Horovitz, A., and Fersht, A. R. (1990) *J. Mol. Biol. 214*, 613−617.
12. Schreiber, G., and Fersht, A. R. (1995) *J. Mol. Biol. 248*, 478−486.

BI002584N